Article

Rhinovirus Uses a Phosphatidylinositol 4-Phosphate/Cholesterol Counter-Current for the Formation of Replication Compartments at the ER-Golgi Interface

Pascal S. Roulin,[1,2] Mark Lötzerich,[1] Federico Torta,[3] Lukas B. Tanner,[3,5] Frank J.M. van Kuppeveld,[4] Markus R. Wenk,[3] and Urs F. Greber[1,*]

[1]Institute of Molecular Life Sciences, University of Zurich, Winterthurerstrasse 190, 8057 Zurich, Switzerland
[2]Life Science Zurich Graduate School, Molecular Life Sciences Program, Zurich, Switzerland
[3]Department of Biochemistry, Yong Loo Lin School of Medicine, National University of Singapore, 28 Medical Drive, Singapore 117456, Singapore
[4]Virology Division, Department of Infectious Diseases and Immunology, Faculty of Veterinary Medicine, University of Utrecht, 3584CL Utrecht, The Netherlands
[5]Present address: Lewis-Sigler Institute for Integrative Genomics, Princeton University, Princeton, NJ 08544, USA
*Correspondence: urs.greber@imls.uzh.ch
http://dx.doi.org/10.1016/j.chom.2014.10.003

SUMMARY

Similar to other positive-strand RNA viruses, rhinovirus, the causative agent of the common cold, replicates on a web of cytoplasmic membranes, orchestrated by host proteins and lipids. The host pathways that facilitate the formation and function of the replication membranes and complexes are poorly understood. We show that rhinovirus replication depends on host factors driving phosphatidylinositol 4-phosphate (PI4P)-cholesterol counter-currents at viral replication membranes. Depending on the virus type, replication required phosphatidylinositol 4-kinase class 3beta (PI4K3b), cholesteryl-esterase hormone-sensitive lipase (HSL) or oxysterol-binding protein (OSBP)-like 1, 2, 5, 9, or 11 associated with lipid droplets, endosomes, or Golgi. Replication invariably required OSBP1, which shuttles cholesterol and PI4P between ER and Golgi at membrane contact sites. Infection also required ER-associated PI4P phosphatase Sac1 and phosphatidylinositol (PI) transfer protein beta (PITPb) shunting PI between ER-Golgi. These data support a PI4P-cholesterol counter-flux model for rhinovirus replication.

INTRODUCTION

Human rhinoviruses (HRVs) are the causative agents of common colds and have a critical role in exacerbations of asthma, chronic obstructive pulmonary disease and cystic fibrosis (Gern, 2010). They set off severe economic burdens, in part, because there are no approved treatments against rhinovirus infections. HRVs are positive-strand RNA viruses from the *Enterovirus* genus of the *Picornaviridae* family that comprises poliovirus, coxsackievirus (CV), enterovirus, or echovirus. Similar to togaviruses, flaviviruses, or picornaviruses, they build up membrane-associated replication complexes in the cytoplasm, composed of lipids, viral and cellular proteins, and replicating RNA (Belov and van Kuppeveld, 2012). In case of hepaciviruses and picornaviruses, the replication complexes form a tubulo-vesicular network of endomembranes with positive curvature.

There are more than 150 HRV types in three species: HRV-A (74 types), HRV-B (25), and HRV-C (55) (Jacobs et al., 2013). HRV-A and HRV-B types are classified into major and minor groups. They use intercellular adhesion molecule 1 or low-density lipoprotein (LDL) family receptors for entry, respectively. The recently discovered HRV-C types use an unknown receptor and are difficult to grow in standard tissue culture. Rhinovirus is composed of an icosahedral capsid enclosing a positive-sense single-stranded RNA genome of about 7,200 nt. It enters cells by receptor-mediated endocytosis and uncoats upon receiving cues from receptor binding and low pH in endosomes (Suomalainen and Greber, 2013). At 30–60 min after endocytic uptake, viral RNA is uncoated and translated into a polyprotein, which is processed by viral proteases into capsid proteins, membrane-associated proteins, and replication proteins, including viral RNA polymerase 3D and proteases 2A and 3C/D. This results in drastic changes in the endomembrane system, in part due to a block in secretion (Sharp and Estes, 2010).

How viral proteins interact with cellular factors and lipids to build up replication membranes is important for both fundamental research and drug development strategies (Heaton and Randall, 2011). For example, phosphatidylinositol (PI) and its phosphorylated derivatives produced by PI kinases (PIK) have key functions in membrane trafficking and signaling. There are two classes of PI 4-kinases (class 2 and 3 PI4K). Class 3 PI4K has been implicated in replication of hepatitis C virus and picornaviruses (Hsu et al., 2010; Reiss et al., 2011; Spickler et al., 2013; van der Schaar et al., 2013). PI4K2a effectively functions on endosomes; PI4K2b is involved in the transmission of stress signals, and producing $PI4,5P_2$ at the plasma membrane and other membranes; and PI4K3a has been implicated in the formation of ER exit sites for cargo export from ER to Golgi (Balla, 2013). PI4K3b regulates membrane traffic within the Golgi and Golgi-to-plasma-membrane transport (Godi et al., 1999). PI4Ks produce PI4P from PI. PI4P effectors at the trans-Golgi-network (TGN) include coat adaptors for vesicular trafficking (such as the

clathrin adaptor 1 and γ-ear-containing Arf-binding proteins) and also soluble lipid transfer proteins, such as oxysterol binding protein 1 (OSBP1) (also known as OSBP), ceramide-binding protein, and four-phosphate adaptor protein 1 and 2.

In this study, we employed targeted RNAi in combination with lipid mass spectrometry and chemical interference to identify host factors controlling processes in lipid metabolism for rhinovirus infection. Our data support a PI4P-cholesterol countercurrent model at ER-Golgi contact sites (Mesmin et al., 2013). We extend this model by showing that HRV-A1A and -A16 infections require PI-transfer protein beta (PITPb). PITPb transfers PI and phosphatidylcholine (PC) between membranes in vitro, localizes to the Golgi, and is required for retrograde transport (Carvou et al., 2010). We also demonstrate that HRV-A16 is dependent on the cholesteryl-esterase hormone-sensitive lipase (HSL), whereas HRV-A1A is more dependent on endosome and Golgi-associated OSBP-like (OSBPL) proteins, such as OSBPL1, L5, L9, and L11, and the lipid droplet (LD)-associated OSBPL2. OSBP1 and OSBPL proteins form a large, evolutionarily conserved family of lipid-binding proteins that mediate sterol signaling and transport between membrane compartments and hence contribute to membrane dynamics and lipid flow. Our data provide a paradigm for ER-Golgi membrane flux in the absence of a functional secretory pathway in rhinovirus infected cells.

RESULTS

The Lipid Kinase PI4K3b Is Required for HRV Replication

HRV serotypes from species A and B require PI4Ks for infection, as suggested by studies with chemical inhibitors (Spickler et al., 2013; van der Schaar et al., 2013). To determine which PI4Ks were required for HRV infection and replication, we used a pool of small interfering RNAs (siRNA) directed against the known PI4Ks. We addressed PI4K2a (PI4K class 2 alpha), PI4K2b, PI4K3a, and PI4K3b and tested effects on replication of five HRVs encompassing HRV-A species (HRV-A1A, HRV-A2, and HRV-A16) and B species (HRV-B14 and HRV-B37). HRV-A16, HRV-B14, and HRV-B37 are ICAM-tropic major rhinoviruses, whereas HRV-A1A and HRV-A2 are LDLR-tropic minor rhinoviruses. In addition, we used the enterovirus Coxsackievirus B3 (CVB3), which requires PI4K3b for replication (Hsu et al., 2010). The knock-down of PI4K3b inhibited the infection with all tested HRV-types and also CVB3 in the range of 31% to 80%, as scored by immunofluorescence high-throughput assay using a double-stranded RNA (dsRNA) antibody (Figure 1A; Figure S1A available online) (Jurgeit et al., 2012; Jurgeit et al., 2010). This was confirmed by western blotting of cell extracts with an antibody against PI4K3b and cytotoxicity assessments by cell number measurements (Figures 1A and 1B). The knock-down of PI4K2a inhibited infection of all HRV-types tested, particularly strongly the minor HRV-A1A and -A2, but not CVB3, possibly highlighting a common endocytic or replication requirement for HRVs. PI4K3a knock-down strongly inhibited infection with minor HRV-A1A and -A2 and also reduced the cell numbers, although this was independent of infection inhibition, suggesting that minor HRV infections require a functional secretory pathway. Although PI4K3a knock-down inhibited infection with minor HRV-A1A and -A2, inhibitors of

PI4K3a activity, such as AL-9, did not affect HRV replication (data not shown; Bianco et al., 2012). PI4K2b knock-down inhibited HRV-A2 but did not inhibit other rhinoviruses or CVB3 (Figures S1A and S1B).

Prior genome-wide RNAi screens suggested that PI4K3b was involved in HRV-A1A and -A16 infection (U.F.G., unpublished results). To further explore a role of PI4K3b in HRV infection, we employed the synthetic PI4K3b inhibitor PIK93. PIK93 inhibits PI4K3b activity with in vitro half inhibitory concentration (IC_{50}) of 19 nM and PI4K3a with IC_{50} of 1 μM (Knight et al., 2006). In both HeLa and primary human airway epithelial cells of nasal biopsies (hAECN), PIK93 blocked infection with all HRV types tested (A1A, A2, B14, A16, and B37) and CVB3 with effective concentrations (EC_{50}) ranging from 170 nM to 915 nM for HRV-A2 and HRV-A1A, respectively (Figures 1C and S1C–S1E). Importantly, PIK93 had minimal effects on metabolic activity (Figure S1F). The PIK93 inhibitory profiles against HRVs corresponded well with the antiviral efficacy of PI4K3b siRNAs and surprisingly showed little effect on HRV-A1A (Figures 1A and 1C). Further tests using RT-PCR for viral RNA measurements, entry bypass assays using genomic RNA transfections, and time-controlled drug additions to cells showed that PIK93 blocked viral replication rather than entry (Figures S1G–S1L). Interestingly, HRV-A1A infection was less sensitive to PIK93 than transfection of viral RNA, suggesting that steps in entry render HRV-A1A relatively insensitive to PIK93, compared to HRV-A16. The specific PI4K3b inhibitor GSK2998533A blocked HRV and CVB3 infections of HeLa cells with EC_{50} values of about 30–100 nM, confirming the role of PI4K3b for HRV infection (Figures S1M and S1L). As expected, all HRVs and CVB3 were strongly inhibited by the fungal metabolite brefeldin A (BFA) (10 μM, Figure 1C).

Cytoplasmic PI4P Levels Are Increased near HRV Replication Sites

We used ion chromatography with suppressed conductivity detection to determine the levels of PI4P in HRV-A1A- and -A16-infected HeLa cells 30 min or 7 hr postinfection (pi). To account for variability in lipid extraction, we normalized the results to the mass of cardiolipin (CL). PIK93 slightly reduced the PI4P levels compared to uninfected control cells, indicating that PI4K3b contributes to maintain the levels of PI4P at steady state (Figure 2A). At 30 min pi, infected cells had reduced levels of PI4P compared to uninfected cells. This decrease correlated with an increase of the $PI4,5P_2$ levels by about 20% independent of PIK93 treatment (data not shown). This suggests that PI4P is converted to $PI4,5P_2$ during HRV entry independent of PI4K3b activity. At 7 hr pi, the PI4P level increased by about 30% in HRV-A1A- or A16-infected cells compared to uninfected cells. This increase in PI4P lipids was not due to enhanced levels of PI4K3b, as shown by western blotting (Figure 2B). It was, however, blunted by PIK93 but without affecting the levels of PI4K3b in HRV-A16 infected cells. The data demonstrate that PI4P lipids are increased at the time of HRV RNA replication owing to PI4K3b activity.

We next investigated the subcellular location of PI4P in digitonin-permeabilized cells using an immunofluorescence-based assay specifically detecting cytoplasmic PI4P. Compared to uninfected cells, the cytoplasmic PI4P signals increased in HRV-A1A- or A16-infected cells, predominantly in the vicinity of newly synthesized VP2 around the nucleus—for example, 8 hr but not
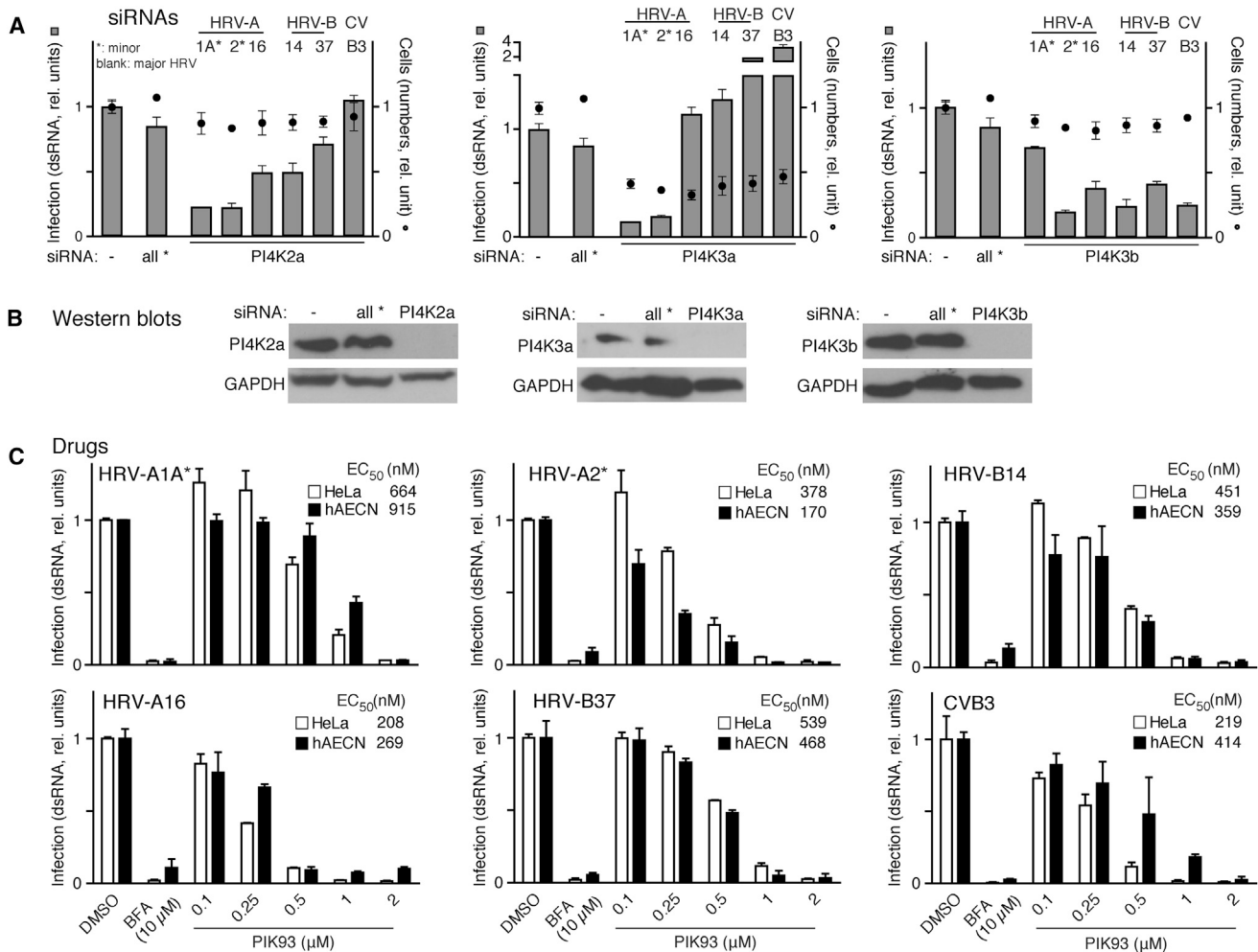
Figure 1. PI4K3b and PI4K3a Support Replication of Rhinoviruses

(A) Effects of siRNAs against PI4K2a, PI4K3a, or PI4K3b (pool of four distinct siRNAs each), or with the negative control siRNA (all star, *) on HRV-A1A, -A2, -A16, -B14, -B37, or CVB3 infection. Minor HRV are denoted by *. Values represent means ± SD, n = 2.

(B) Western blots of lysates from HeLa cell infected with HRV-A16 (MOI 50) probed with antibodies against PI4K2a, PI4K3a, PI4K3b, or glyceraldehyde-phosphate dehydrogenase (GAPDH).

(C) Drug treatments of HeLa (white bars) or hAECN (black bars) 1 hr prior to infection, including DMSO, brefeldin A (BFA), and PIK93. EC_{50} values of inhibitors on infections (8 hr for HeLa, or 18 hr for hAECN) were obtained by nonlinear regression of the data fitted to the variable-slope sigmoidal dose-response. Values represent means ± SD, n = 2. Refers to Figure S1.

1 hr pi (Figures 2C and 2D). We also found that PI4K3b localized in the proximity of replicated viral RNA by immune staining PI4K3b and dsRNA (Figure 2E). Interestingly, a small amount of dsRNA-positive foci dispersed from the bulk was found to be PI4K3b negative. In uninfected cells, PI4K3b colocalized with the peripheral cytoplasmic TGN marker p230 and the *cis*-Golgi marker GM130 but not the ER marker calnexin (Figure 2F). In infected cells, newly synthesized VP2 colocalized with p230, GM130, and the ER-Golgi intermediate compartment marker ERGIC53 in perinuclear clusters of punctate fluorescence (Figures S2A–S2C). Intriguingly, the perinuclear VP2-positive areas appeared to be enriched in calnexin, suggesting that HRV infection reorganized cellular compartments (Figure S2D).

To test a functional involvement of the TGN, we subjected the cells to Exo2, a small compound disrupting the TGN and early endosomes but not the ER or ERGIC (see Figure S2E) (Spooner et al., 2008). Exo2 is more specific than BFA, which disrupts the TGN and also the *cis*-Golgi (Figure S2E). Exo2 blocked HRV-A1A and -A16 replication in a dose-dependent manner with EC_{50} between 16.2 and 24.6 μM, if added prior to 3 hr pi, suggesting an involvement of the TGN in HRV replication (Figure S2F). Together, the data show that PI4P lipids are produced by PI4K3b in the vicinity of HRV replication sites near Golgi and ER compartments, and viral replication requires the TGN.

HRV Infected Cells Increase Cholesterol and Reduce Cholesteryl-Esters

Cells infected with enteroviruses, including rhinoviruses, display high levels of positively curved cytoplasmic membranes, as indicated by thin section electron microscopy (EM) (see Figure 3A).

A Total PI4P:
Ion chromatography with suppressed conductivity detection

30 min p.i. | DMSO | PIK93
7 h p.i.

Ratio PI4P / CL

not infected   HRV-A1A   HRV-A16

B

HRV-A16:	-	UV	+	+	+	+	+	+
treatment:	-	-	-	DMSO	BFA		PIK93 (μM)	
						0.25	0.5	1

PI4K3b

GAPDH

| PI4K3b / GAPDH | 1.00 ± 0.00 | 1.05 ± 0.06 | 0.95 ± 0.10 | 0.98 ± 0.11 | 0.94 ± 0.07 | 1.11 ± 0.24 | 0.92 ± 0.13 | 0.85 ± 0.07 |

C
not infected VP2   Cytoplasmic PI4P   Cytoplasmic PI4P VP2 DAPI

HRV-A1A

HRV-A16

single sections

E
not infected dsRNA   PI4K3b   PI4K3b dsRNA DAPI

HRV-A1A

HRV-A16

single sections

D Perinuclear PI4P: Fluorescence microscopy

1 h p.i.

Perinuclear PI4P (rel. units per area)

n=52
1.0 ± 0.3

n=36
1.4 ± 0.6

n=42
0.8 ± 0.4

not infected   HRV-A1A   HRV-A16

8 h p.i.

n=48
4.5 ± 1.5

n=41
5.2 ± 1.8

n=54
1.0 ± 0.4

not infected   HRV-A1A   HRV-A16

max. projections   PI4P DAPI

F
not infected p230   PI4K3b   PI4K3b p230 DAPI

not infected GM130   GM130

not infected calnexin   calnexin

single sections

Figure 2. PI4P and PI4K3b Are Enriched on Rhinovirus Replication Sites
(A) Total lipids extraction and PI4P measurement by ion chromatography with suppressed conductivity detection from HeLa cells treated with DMSO or 1 μM PIK93 1 hr prior to infection with HRV-A1A or HRV-A16 (MOI 50). Values were normalized to CL and represent means ± SD, n = 3.
(B) No gross reduction of PI4K3b levels detected by western blotting upon treatment of cells with PIK93 inoculated with HRV-A16 or UV-treated HRV-A16 (MOI 50) for 8 hr. Values are means ± SD, n = 3.
(C) HeLa cells infected with HRV-A1A or HRV-A16 (MOI 20) for 8 hr were stained for viral protein VP2 (green), cytoplasmic PI4P (red), and nuclei with DAPI (blue). Scale bar: 10 μm.
(D) HeLa cells infected with HRV-A1A or HRV-A16 were stained for cytoplasmic PI4P (green) and nuclei (blue). The total intensity of perinuclear PI4P signal for each cell was measured and normalized to the corresponding area. Values are means ± SD, n ≥ 36.
(E and F) HeLa cells infected with HRV-A1A or HRV-A16 (8 h) were stained for dsRNA (green), PI4K3b (red), and DAPI (nuclei, blue). Noninfected cells were stained for p230, GM130 or calnexin (green), and PI4K3b (red). Scale bar: 10 μm. Refers to Figure S2.

But how these membranes receive their lipids has been incompletely explored. Toward elucidating if cholesterol was involved in HRV replication, we analyzed the levels of cholesterol by fluorescence microscopy and mass spectrometry. Cholesterol staining with filipin revealed a striking colocalization with VP2 in perinuclear clusters of HRV-A1A- or A16-infected cells 8 hr pi (Figure 3B). Fluorescence quantification showed a significant increase in the perinuclear filipin signal 14 hr pi, and a trend to increase 8 pi, albeit less pronounced in HRV-A1A- than HRV-A16-infected cells (Figure 3C). These results were confirmed by mass spectrometry in cell populations, showing that population levels of cholesterol increased from 140 μg/ml before infection to 190–220 μg/ml at 7, 15, or 22 hr pi with HRV-A16, although not significantly with HRV-A1A compared to uninfected cells (Figures 3D and S3A). Concomitantly, the levels of cholesteryl-esters were found to be reduced from 60 or 85 μg/ml before infection to 33 or 56 μg/ml 15 or 22 hr pi in HRV-A1A or HRV-A16 infected cells, respectively. This suggests that cholesteryl-esters contribute to increase cholesterol pools in rhinovirus infected cells, although they may not be sufficient to cover the entire surge in cholesterol in HRV-A16 infected cells.

Distinct mechanisms can increase the levels of cholesterol in the ER membrane. One is de novo biosynthesis from acetyl CoA through the mevalonate pathway on ER membranes, including the rate limiting enzyme 3-hydroxy-3-methylglutaryl-coenzyme A (HMG-CoA) reductase. A second one is uptake of extracellular cholesterol via late endosomes, or third, hydrolysis of cholesteryl-esters in LDs or late endosomes (Ikonen, 2008). To determine whether de novo biosynthesis was required for HRV replication, we tested the effect of small chemical inhibitors of cholesterol metabolism on HRV infection and replication (Figure 3E). HeLa cells were infected with HRV-A1A or -A16 at multiplicity of infection (MOI) 20; treated with compounds, and stained by anti-VP2 antibodies 8, 10, 12 or 14 hr pi or were analyzed for replication of viral RNA by quantitative RT-PCR. 25-HC is produced from cholesterol by cholesterol 25-hydroxylase, inhibits one of the rate limiting enzymes in cholesterol biosynthesis HMG-CoA reductase (Kandutsch and Chen, 1974), and also blocks OSBP1 (Mesmin et al., 2013; Wang et al., 2008). 25-HC strongly inhibited HRV-A1A and HRV-A16 infection and replication, comparable to PIK93 (Figures 3F, 3G, 1E, and 1F). 25-HC also inhibited the expression of HMG-CoA reductase mRNA in uninfected cells to levels similar as in infected cells not treated with compound (Figure 3H). In addition, 25-HC and methyl-β-cyclodextrin (MβCD), which depletes cells of cholesterol by extracting free cholesterol from membranes, inhibited HRV-A1A or -A16 infections under conditions, where the inoculum was washed off the cells 1 hr pi, compounds added 2 hr pi, and infection scored 8 or 14 hr pi (Figure S3B). These results were similar to PIK93 and highlight that cholesterol is required for one or several postentry steps in HRV infection and replication. In contrast, compactin or AY9944, which inhibit cholesterol biosynthesis at early or late steps by blocking HMG-CoA reductase, or Δ⁷-dehydrocholesterol reductase, respectively, had relatively little effect, since the drug treatments led to 10%–30% reduction in HRV-A16 and 50% reduction in HRV-A1A infection at 8 hr pi, but no effects were visible anymore at 10, 12, or 14 hr pi (Figures 3F–3H). Neither MβCD, AY9944, nor compactin showed adverse toxicity in the resazurin metabolic assay (Figure S3C). As expected, the cholesterol biosynthesis inhibitors compactin (10 μM) or AY9944 (10 μM) did not reduce but rather increased the expression of HMG-CoA reductase. Likewise, these compounds did not inhibit HRV infection of hAECN, as measured by dsRNA immunofluorescence (data not shown). The data suggest that cholesterol biosynthesis has little role in HRV replication, although cholesterol crucially supports replication.

HRV Infections Cluster Lipid Droplets near Replication Centers and Require Hormone Sensitive Lipase

To further explore the mechanism of cholesterol increase in rhinovirus-infected cells, we investigated if LDs were involved in infection. LDs contain neutral lipids such as cholesteryl-esters or triacylglycerol and a monolayer of phospholipids, as well as a key set of proteins (Walther and Farese, 2012). Compared to uninfected cells, the size and shape of LDs stained with LD540 and scored by fluorescence microscopy did not significantly change in infected cells 8 hr pi (Figures 4A and 4B). At 14 hr pi, however, fewer and bigger LDs were detected, and some of them colocalized with puncta of newly synthesized VP2.

We determined if hydrolysis of cholesteryl-esters was implicated in HRV infection by treating cells with an inhibitor of HSL which catalyzes the hydrolysis of cholesteryl-esters, tri-, di-, and monoacyl-glycerols and is associated with LDs. The pretreatment of cells with the HSL inhibitor CAY10499 reduced HRV-A1A and -A16 infections in a dose-dependent manner with EC₅₀ of 0.35 and 5.2 μM at 8 hr pi (Figure 4C). Addition of CAY10499 to cells after infection decreased HRV inhibition less effectively (EC₅₀ values between 4 and 92.9 μM) depending on the HRV type and the time of addition (Figure 4D). This was in accordance with the report that the inhibition of HSL cholesteryl-esterase activity with CAY10499 required prolonged inhibitor pretreatment (Manna et al., 2013). Importantly, CAY10499 was not toxic up to 64 μM (Figure 4E). In addition, RNA interference against HSL significantly inhibited replication of HRV-A16 but not HRV-A1A (Figures 4F–4H). The data show that some rhinoviruses take advantage of host lipases to produce cholesterol from cholesteryl-esters and thereby enhance replication on Golgi-derived membranes.

To address how HRV-A1A accesses cholesterol, we conducted an siRNA miniscreen against OSBP-like proteins (OSBPLs), also called OSBP-related proteins (ORPs). OSBPLs are intracellular sterol sensors or transporters, frequently located at membrane contact sites (Olkkonen and Li, 2013). Strikingly, HRV-A1A was inhibited by RNAi against OSBPL1, L2, L5, L6, L7, L8, L9, L10, and L11, but not L3 or L4, while the other rhinoviruses and CVB3 were less dependent on OSBPLs (Figure 4H and S4A–S4D). OSBPL1, L2, and L5 are implicated in ER-late endosomes or ER-LDs contacts, and L3 and L4 in ER-plasma membrane contact sites (Olkkonen and Li, 2013). Notably, OSBPL2 is associated with LDs, and its knockdown increases cholesteryl-ester synthesis (Hynynen et al., 2009) and thereby could inhibit HRV-A1A infection. OSBPL5, which is located on the ER, has been implicated in cholesterol exit from late endosomes and lysosomes (Du et al., 2011). Interestingly, OSBPL9 and L11 were involved not just in HRV-A1A but also -A2, -B14, and -A16, but not -B37 or -CVB3, infections and localized near HRV-A1A or -A16 replication sites (Figure S4A). OSBPL11 pairs
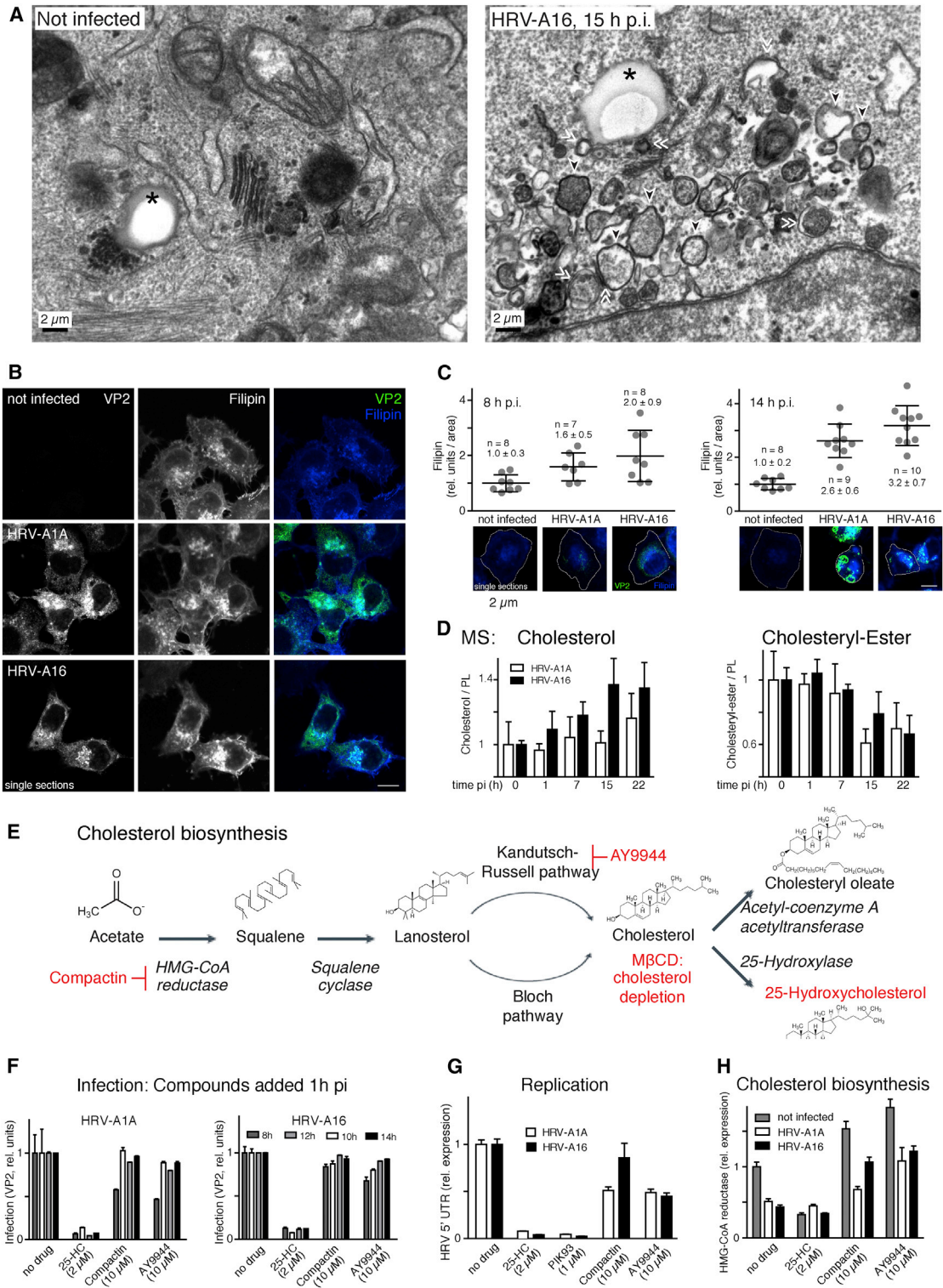
Figure 3. Cholesterol Is Enriched on HRV Replication Sites

(A) Electron micrographs of HeLa cells infected with HRV-A16 (MOI 1), or uninfected cells, Epon embedded and stained with uranyl acetate. Positively curved viral replication membranes are shown by arrow heads; areas with multiple membranes closely apposed are highlighted by double arrow heads, and lipid droplets indicated by *.

(B) HeLa cells infected with HRV-A1A or HRV-A16 for 8 hr were stained for VP2 (green) and cholesterol (blue). Scale bar: 10 μm.

(C) Quantification of filipin signal representing total cholesterol for each cell normalized to its area. Values are means ± SD, n ≥ 7.

(legend continued on next page)

with OSBPL9 and localizes at the Golgi-endosome interface (Olkkonen and Li, 2013). Together the data suggest that late endosomes can supply cholesterol for rhinovirus replication. For HRV-A1A, an involvement of late endosomes may compensate for LD-associated cholesteryl-ester hydrolysis.

The PI4P-Cholesterol Exchange Protein OSBP1, VAP-B, Sac1, and PITPb Are Required for HRV Replication

Several lines of evidence pointed to an involvement of the PI4P-cholesterol exchange protein OSBP1 in HRV infection, namely the increase in both PI4P and cholesterol levels at stages of viral replication, the sensitivity of HRV infection to 25-HC, and the infection independence of cholesterol biosynthesis. The latter supported the notion that 25-HC inhibited HRV infection by blocking OSBP1. In accordance with this, the treatment of cells with 25-HC induced the clustering of OSBP1 in perinuclear Golgi-like areas (Figure S5A). This was consistent with the finding that 25-HC not only blocks the ability of OSBP1 to extract sterols from the ER through its lipid transport domain (ORD) but also extraction of PI4P from the Golgi, and hence leads to accumulation of OSBP1 at Golgi-ER interface (Mesmin et al., 2013; Wang et al., 2008).

We determined the EC_{50} for 25-HC-mediated enterovirus infection inhibition in HeLa and primary cells for HRV-A1A, -A2, -B14, -A16, B37, and CVB3. For HRV-A types, 25-HC EC_{50} were below 1 μM, for the B-types close to 1 μM, and for CVB3 about 4 μM without metabolic toxicity (Figures 5A–5C and S5A–S5E). In hAECN cells, the EC_{50} values for 25-HC were around 1 μM for the HRV-A types and around 2 μM for the HRV-B types (Figures 5C and S5D). 25-HC did not inhibit CVB3 replication in hAECN cells up to 10 μM and did not affect the metabolic activity of cells up to 10 μM during 8 or 24 hr periods of incubation (Figure 5B). Time course addition experiments showed that 25-HC addition at 1 or 3 hr pi was nearly as effective at inhibiting HRV-A, HRV-B, or CVB3 as when added prior to infection, although the EC_{50} were slightly higher upon addition pi (Figures 5D and S5F). This shows that 25-HC has minor effects on steps prior to replication. When added 5 hr pi at the onset of replication, however, 25-HC did not inhibit infections, indicating that it blocked initiation of the viral replication membranes.

To further test if OSBP1 is specifically required for HRV replication, we knocked down OSBP1 by RNAi. OSBP1 knockdown was very efficient and inhibited infection with all HRV types tested and CVB3, although the effects on HRV-B14, -B37, and CVB3 were not as pronounced as on HRV-A1A, -A2, and -A16 (Figures 5E and 5F). This provides strong evidence that OSBP1 broadly enhances enterovirus infection. OSBP1 is an 807 aa

multidomain protein with an N-terminal PH domain, a FFAT (two phenylalanines in an acidic track) motif, and a C-terminal ORD domain (Figure 5G). It localizes at ER-Golgi contact sites by binding simultaneously Golgi PI4P through its PH domain and the ER vesicle-associated membrane protein (VAMP)-associated protein A or B (VAP-A or VAP-B, respectively) via its FFAT motif. Expression of FLAG (phenylalanine-leucine-alanine-glycine)-tagged OSBP1 in uninfected cells showed a tight localization of the protein in a perinuclear area, reminiscent of Golgi localization (Figure 5H) (Amako et al., 2009). In HRV-A1A- or A16-infected cells, FLAG-OSBP1 was more dispersed than in uninfected cells and localized to areas positive for VP2, for example, 8 hr pi. An OSBP mutant lacking the PH domain (ΔPH-OSBP1) was distributed throughout the cytoplasm but not on the Golgi. Its expression led to a clear reduction of VP2 signals, suggesting that it reduced infection by acting as a dominant-negative protein interfering with the function of the endogenous OSBP1, possibly displacing endogenous OSBP1 from VAP-B. Strikingly, ΔPH-OSBP1 did not colocalize with VP2, indicating that the PH domain binding to PI4P was crucial for the recruitment of OSBP1 to newly synthesized VP.

OSBP1 and also yeast Osh4p shuttle cholesterol against a concentration gradient of cholesterol from the ER to the Golgi, and this involves the ER-associated OSBP1 binding protein VAP-A, the ER-associated PI4P phosphatase Sac1, and the PI-transfer protein PITPb (de Saint-Jean et al., 2011; Mesmin et al., 2013; Olkkonen and Li, 2013). The driving force for cholesterol shuttling against its concentration gradient comes from shuttling PI4P along its concentration gradient from Golgi to ER, at ER-Golgi contact sites. Using RNAi, we found that the knockdown of VAP-B, Sac1, or PITPb inhibited infection with HRV-A1A and -A16, as measured by dsRNA high-throughput fluorescence microscopy or western blotting with an antibody against VP2, which also detects the viral polyprotein precursor VP0 (Figures 5I and 5J). The data support a model where a cycle of PI4P, cholesterol, and PI lipids between the ER and the Golgi drives the replication of rhinovirus on Golgi membranes in close proximity to the ER.

DISCUSSION

How different lipid species act together to build up viral replication compartments is poorly understood. We analyzed host factors controlling the flux of the phosphoinositide PI4P and the neutral lipids cholesterol and cholesteryl-esters in rhinovirus-infected cells (Figure 6A). Increased levels of PI4P were found on Golgi membranes of infected cells by virtue of PI4K3b, and cholesterol was increased near viral replication sites. The lipid

(D) Quantification of cholesterol and cholesteryl-esters by mass spectrometry normalized to the phospholipid (PL) in HRV-A1A- and HRV-A16-infected cells (MOI 50). Values are means ± SD, n = 3.

(E) Depiction of the cholesterol biosynthesis pathway with the limiting-rate HMG-CoA reductase and inhibitors of early and late cholesterol biosynthesis (compactin and AY9944, respectively), the cholesterol-depleting agent (MβCD), and the OSBP1 ligand 25-HC depicted in red.

(F) Infection profiles of HeLa cells infected with HRV-A1A or HRV-A16 in presence or absence of 25-HC, compactin, or AY9944 added 1 hr pi. The ratio of infected cells was calculated and normalized to the mock control. Values are means ± SD, n = 2.

(G) Viral replication measured by RT-PCR of HRV 5′ UTR in HeLa cells infected with HRV-A1A or HRV-A16 (8 hr) and treated with 25-HC, PIK93, compactin, or AY9944 1 hr prior to infection. Data are normalized to the respective geometric means of GAPDH, transferrin receptor (TRFC), and eukaryotic elongation factor (EEF).

(H) Reduction of HMG-CoA reductase expression in HRV-A1A- or HRV-A16-infected cells measured by RT-PCR normalized to the respective geometric means of GAPDH, TRFC, and EEF. Values are means ± SD, n = 3. Refers to Figure S3.

A 8 h p.i. — Lipid droplets — 14 h p.i.

B LD numbers — LD area — 8 h p.i. — 14 h p.i.

C Pre-treatment 8 h p.i.

EC$_{50}$ (μM)
HRV-A1A 5.20
HRV-A16 0.35

D Post-treatment

HRV-A1A
EC$_{50}$ (μM)
+1 h p.i. 9.47
+3 h p.i. 20.5
+5 h p.i. 92.9

HRV-A16
EC$_{50}$ (μM)
+1 h p.i. 4.00
+3 h p.i. 20.3
+5 h p.i. 73.5

E Metabolic activity

F RNAi

G Western blots: HRV-A16 infected cells
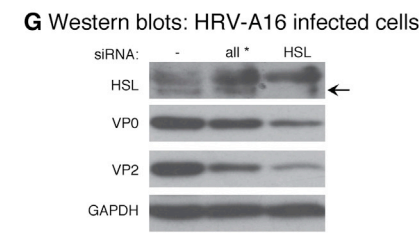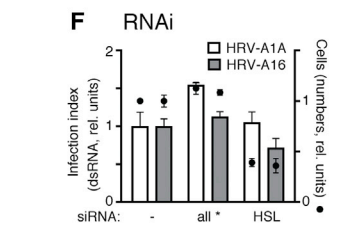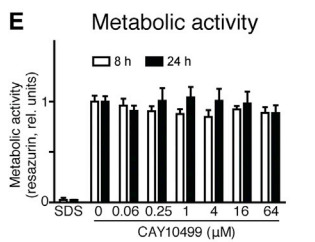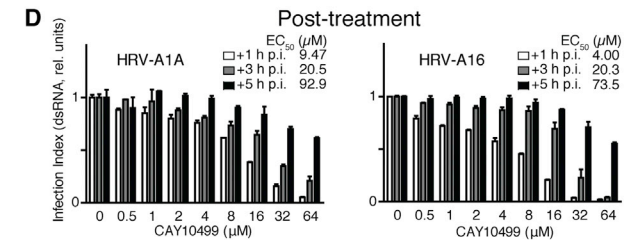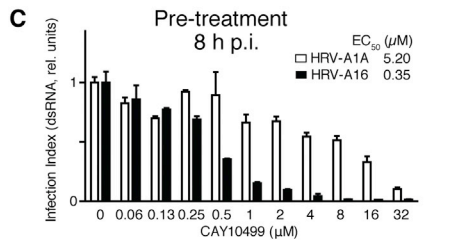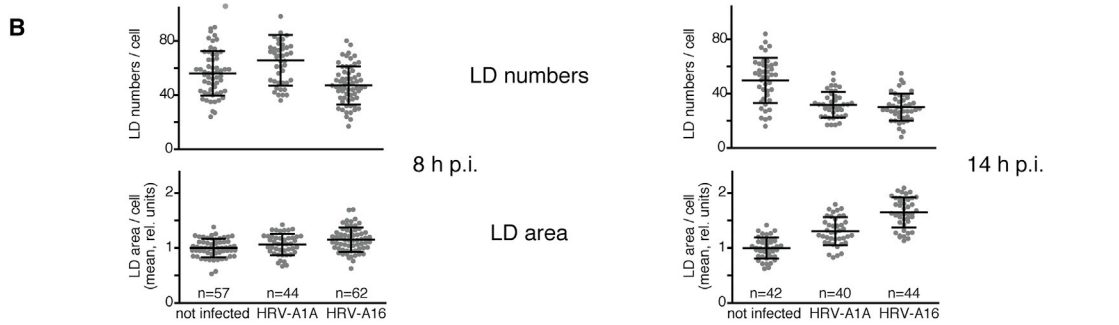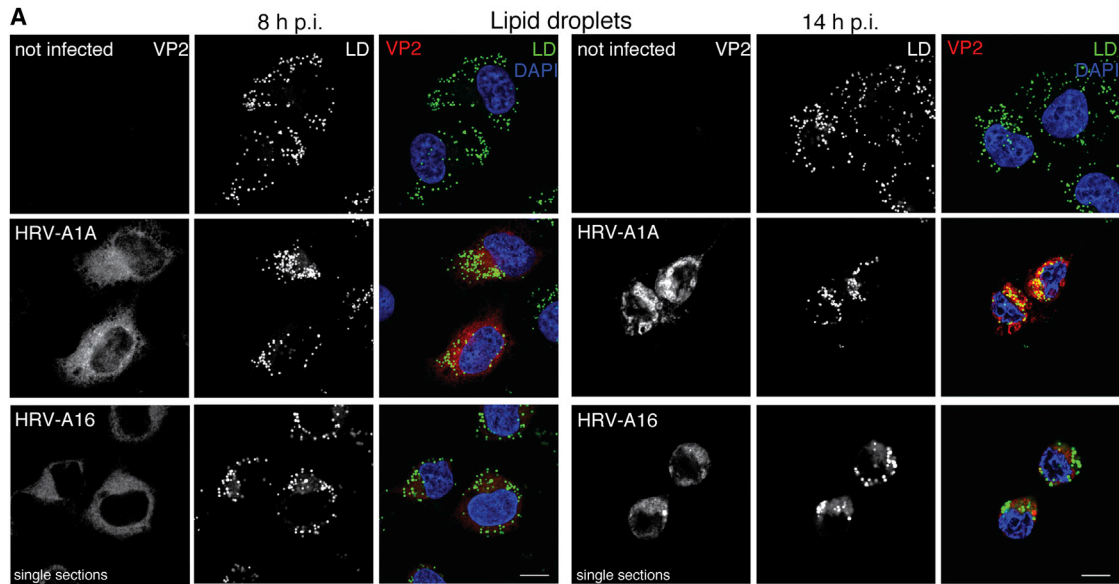
H RNA interference (+ denotes > 50% infection inhibition by immuno-fluorescence of dsRNA)

	OSBPL1	OSBPL2	OSBPL5	OSBPL6	OSBPL7	OSBPL8	OSBPL9	OSBPL10	OSBPL11
HRV-A1A*	+	+	+	+	+	+	+	+	+
HRV-A2*	+	-	+	+	-	-	+	+	+
HRV-A16	-	-	-	+	-	-	+	-	+
HRV-B14	-	-	-	-	-	+	+	-	+
HRV-B37	-	-	-	-	-	-	-	-	+
CVB3	-	-	-	-	-	-	-	-	-

*: minor   blank: major HRV

(legend on next page)

transfer protein OSBP1 exchanges PI4P with cholesterol at membrane contact sites and is broadly required for rhinovirus replication, as well as the ER phosphatase Sac1 hydrolyzing PI4P, presumably to preclude PI4P competition for sterol binding on OSBP1.

We also show that rhinovirus-infected cells utilize cholesteryl-esters from LDs or late endosomes to produce cholesterol, which is key for replication. Our model depicted in Figure 6B extends a recently proposed one-to-one counter-current sterol to PI4P gradient model for forward trafficking of sterols from the ER to the Golgi (de Saint-Jean et al., 2011; Mesmin et al., 2013). Lipid flux between adjacent membrane compartments may be akin to treadmilling of polymer subunits in cytoskeletal filaments. Yet, the PI4P-cholesterol flux likely involves the coupling of additional lipids in rhinovirus replication, such as PC through PITPb. This may enhance the complexity of lipids building up the membranous web for the replication of positive-sense RNA viruses. These lipids likely codetermine membrane curvature, dynamics, and recruitment of effector proteins, including viral polymerase, or may simply counteract the loss of secretory membrane flux imposed by viral proteins.

Rhinovirus Replication Is Initiated on Golgi Membranes

We show that a range of rhinoviruses require Golgi membranes and PI4K3b to establish their replication sites in the proximity of the TGN, the ER, and the ERGIC, in line with other enteroviruses, such as poliovirus, and CVB3 (Belov and van Kuppeveld, 2012; Hsu et al., 2010; Spickler et al., 2013). HRV replication critically depended on the activity of PI4K3b. PI4K3b was not increased during HRV replication but recruited to sites of RNA replication where it increased the pool of PI4P lipids. Both HRV-A1A and -A16 upregulated PI4P lipids, and this was blunted by the PI4K3b inhibitor PIK93, which is known to block replication of HRV-A, -B, and -C types (Mello et al., 2014; Spickler et al., 2013). The data also provide validation for an emerging antiviral concept, namely to blunt virus-induced cellular activities by inhibiting but not eliminating host factors, thereby gaining antiviral efficacy with minimal collateral damage.

We also found that rhinovirus infection depended on PI4K2a, which localizes to the TGN and endosomes and participates in vesicular trafficking between endosomes and TGN (Wang et al., 2003). Using population measurements in presence of PIK93, PI4K2a activity was apparently not increased in infection, raising the possibility that PI4K2a controls a constitutive pro-

cess, possibly virus uptake into cells, and may not globally induce PI4P levels to support infection. This does not exclude a local induction of PI4K2a activity, for example, similar to the entry of adenovirus, which activates about 3% of the total cellular pool of protein kinase A (Suomalainen et al., 2001). Interestingly, PI4K3a, which controls the formation of ER exit sites (Farhan et al., 2008), supported infection with the minor HRV-A1A and -A2 types and could be involved in the entry or replication of LDL-receptor tropic HRVs.

Cholesterol and Cholesteryl-Esters Are Crucial for HRV Replication

Rhinovirus-infected cells have high levels of positively curved cytoplasmic membranes, similar to other enteroviruses. Cholesterol insertion into a lipid bilayer determines the equilibrium curvature and increases bending stiffness of membranes (Bruckner et al., 2009). One possibility for acquiring cholesterol is receptor-mediated endocytosis, as suggested for poliovirus and CV (Ilnytska et al., 2013). HRV replication was not inhibited by the knockdown of Rab5, Rab11, DAB2, HIP1, or Epsin15L, but Rab18 knockdown, which affects the formation of lipid droplets, reduced HRV infection (data not shown). We observed increased levels of cholesterol at sites of replication, although HRV-A1A did not increase the overall cholesterol levels in cells, unlike HRV-A16.

A major fraction of cholesterol increase correlated with a reduction of cholesteryl-esters for both HRV-A1A and -A16 and was at least in part due to the cholesteryl-esterase HSL. Notably, mass balance considerations indicated that the decrease in cholesteryl-esters unlikely accounts for the full increase in cholesterol in HRV-A16-infected cells. Interestingly, HSL is associated with LDs particularly upon activation of lipolysis, and hydrolyzes a broad range of cholesteryl esters, triglycerides, and lipoidal esters (Hashimoto et al., 2012), which could be used to synthesize cholesterol as long as HMG-CoA reductase is available in cells. In fact, we found that LDs coalesced near the rhinovirus replication sites indicating their mobilization. Interestingly, HRV-A1A infection, which occurs through late endosomes was weakly inhibited by CAY10499 (EC$_{50}$ 5.2 μM versus 0.35 μM for HRV-A16) and was not sensitive to knockdown of HSL, raising the possibility that cholesteryl-esters from other organelles than LDs are recruited for HRV-A1A replication. Strikingly, OSBPL1 (also known as ORP1L) and OSBPL5 were required for infection with LDL-receptor-dependent

Figure 4. Lipid Droplets Are a Source of Cholesterol Source for HRV-A16 Replication

(A) HeLa cells infected with HRV-A1A or HRV-A16 were stained for lipid droplets (LD = green), VP2 (red), and nuclei (DAPI, blue). Scale bar: 10 μm.

(B) CAY10499, an inhibitor of LD-associated cholesteryl-esterase inhibits HRV-A16 and to a lesser extent HRV-A1A. Infection was scored by determining the ratio of infected cells normalized to uninfected controls. EC$_{50}$ values were obtained by nonlinear regression of the data fitted to the variable-slope sigmoidal dose-response. Values are means ± SD, n = 2.

(C and D) Pre- rather than post-entry addition of CAY10499 inhibits infection with HRV-A16 and to a lesser extent HRV-A1A. Infection and EC$_{50}$ values were determined as described in (B). Values are means ± SD, n = 2.

(E) CAY10499 does not affect the metabolic activity of cells up to 64 μM compared to DMSO solvent and 0.01% SDS (positive control) upon treatments as determined by resazurin assays. Values are means ± SD, n = 4.

(F) Knockdown of HSL with a pool of four siRNAs inhibits HRV-A16 but not HRV-A1A infection compared with the negative control siRNA (all star). Values: mean ± SD, n = 2.

(G) Western blots against HSL from lysates of HeLa cells infected with HRV-A16 (MOI 50, 8 hr), including the VPs VP0 and VP2 (mab 16-7, Jurgeit et al., 2010) and GAPDH.

(H) RNAi against OSBPL proteins differentially affects infection with HRV-A1A, -A2, -B14, -A16, -B37, and CVB3, as indicated by dsRNA infection readout in high-throughput microscopy assays 8 hr pi. Minor HRV are denoted by *. Related to Figure 4.
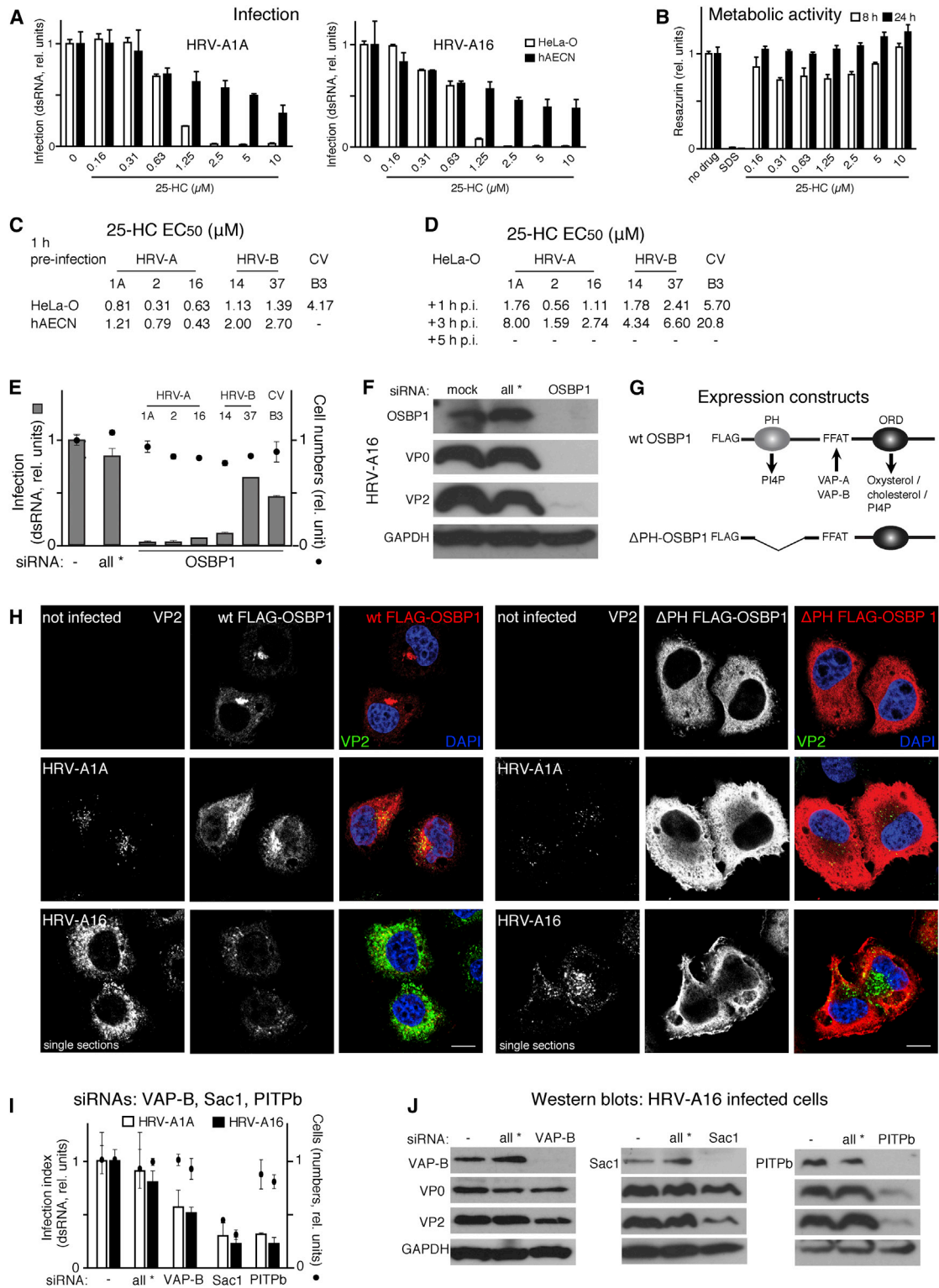
Figure 5. OSBP1 Broadly Supports Enterovirus Infections

(A) 25-HC blocks HRV-A1A and -A16 infections of HeLa or hAECN cells measured by dsRNA immunofluorescence.

(B) 25-HC does not affect the cell metabolic activity measured by resazurin assay. Values are means ± SD, n = 4.

(C) EC_{50} values for 25-HC against HRV or CVB3 infections of HeLa or hAECN cells upon pretreatment of cells. Means ± SD, n = 2.

(D) EC_{50} values for 25-HC added 1, 3, or 5 hr pi. Means ± SD, n = 2.
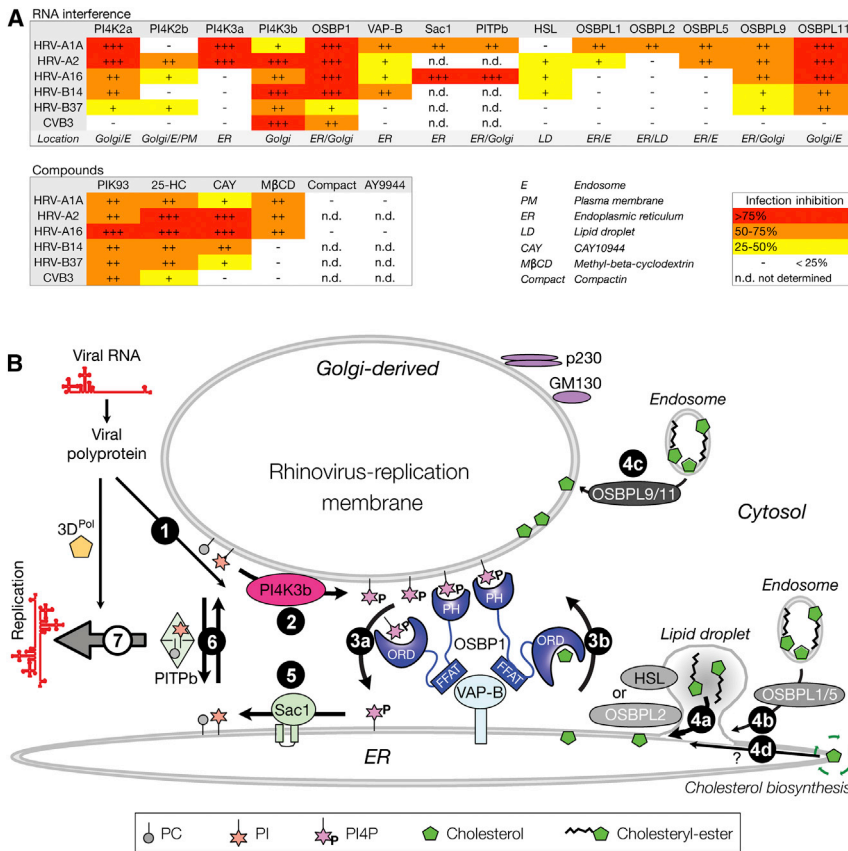
Figure 6. The PI4K3b-OSBP1-Sac1-PITPb Cycle Is Fueled by Storage Cholesterol and Drives Rhinovirus Replication

(A) Model for host factors and inhibitor profiling data for HRV replication (this study), including location of PI4Ks and OSBPL proteins (Balla, 2013; Carvou et al., 2010; Manna et al., 2013; Mesmin et al., 2013; Olkkonen and Li, 2013).

(B) Lipid counter-current flux for rhinovirus replication. (1) Tethering or activation of PI4K3b to Golgi membranes by one or several viral membrane associated proteins. (2) Production of PI4P lipids on the Golgi. (3) Nonvesicular transport of PI4P from Golgi to ER and cholesterol from ER to Golgi through OSBP1. (4) Hydrolysis of cholesteryl-esters from LDs associated with ER (4a) or late endosomes ([4b] and [4c]), and minor contribution from newly synthesized cholesterol (question mark, [4d]). (5) Hydrolysis of PI4P to PI in the ER. (6) Transport of PI from ER to Golgi through the PI transfer protein PITP-b. (7) These events support viral RNA replication and involve RNA-dependent RNA polymerase 3D.

and VAP through its FFAT domain, and thereby functions as a nonvesicular cholesterol transporter equilibrating free cholesterol and PI4P between the ER and the Golgi (Goto et al., 2012; Mesmin et al., 2013). A PH-domain-deleted OSBP1 mutant was not found near viral replication sites but inhibited rhinovirus infection, highlighting the importance of OSBP1 binding to PI4P. In addition, OSBP1 integrates cholesterol levels with cell growth (Raychaudhuri and Prinz, 2010). Under conditions of abundant cholesterol, it sequesters protein phosphatases and thereby derepresses MAP kinase signaling and cell growth, or it functions as a sterol-dependent transducer in cytokine signaling through signal transducer and activator of transcription-3 (STAT3) and Janus-activated kinase-2, which phosphorylates OSBP1 and renders it a scaffold for binding STAT3 (Romeo and Kazlauskas, 2008). The engagement of OSBP1 at cholesterol-rich replication sites could thus tune the cytokine response to rhinovirus infection.

OSBP1 is a target of natural and synthetic compounds with therapeutic potential (Burgett et al., 2011). The oxysterol variant 25-HC binds with higher affinity to OSBP1 than cholesterol, locks OSBP1 in a lipid exchange-inactive state, and inhibits replication of rhinoviruses and also CVB3. This was similar to a

HRV-A1A and -A2, suggesting a role of late endosomal cholesterol for minor HRVs. OSBPL1 can simultaneously bind Rab7 and VAP on late endosomes and the ER, respectively, and thereby contribute to the formation of membrane contact sites (Rocha et al., 2009). It may assist the recruitment of cholesterol from late endosomes. In addition, OSBPL11 knockdown strongly inhibited HRV but not CV replication. OSBPL11 contains a PH domain that binds to PI4P, and can dimerize with OSBPL9, which is located at ER and Golgi membranes. We speculate that HRV recruits additional cholesterol via OSBPL11 independent of OSBP1.

OSBP1 Is a Key Effector of PI4P and Cholesterol Flux and Drives Rhinovirus Replication

OSBP1 plays a central role in enterovirus infection. It is found at membrane contact sites, in particular between the ER and Golgi where it binds PI4P and Arf1-GTP through a PH domain,

(E) RNAi against OSBP1 (pools of four individual siRNAs) compared to the negative control siRNA (all star) inhibits rhinovirus and to a lesser extent CVB3 infection of HeLa cells. Values are means ± SD, n = 2.

(F) Western blots against OSBP1 from lysates of HeLa cells infected with HRV-A16 (MOI 50, 8 hr), including blots against VP0, VP2, and GAPDH.

(G) Schematic depiction of OSBP1 containing a PH domain that binds PI4P and Arf1-GTP on Golgi membranes, an FFAT motif that binds VAP proteins on ER membranes, and an OSBP-related ligand-binding domain (ORD) that shuttles cholesterol and PI4P between membranes.

(H) Immunofluorescence analyses of FLAG-tagged OSBP1 or PH-domain lacking FLAG-OSBP1 (ΔPH FLAG-OSBP) expressed in HeLa cells infected with HRV-A1A or -A16 (8 hr). VP2 staining (green), FLAG-tagged OSBP1 (red), and nuclei (DAPI, blue). Scale bar: 10 μm.

(I) RNAi against VAP-B, Sac1, or PITP-b (pools of four individual siRNAs each) compared to the negative control siRNA (all star) inhibits HRV-A1A and -A16 infection of HeLa cells (8 hr). Values are means ± SD, n = 2.

(J) Western blots against VAP-B, Sac1, and PITPb from lysates of HeLa cells infected with HRV-A16 (MOI 50, 8 hr), including blots against VP0, VP2, and GAPDH. Refers to Figure S5.

report for poliovirus (Arita et al., 2013). 25-HC activates interferon response and has innate antiviral effects (Blanc et al., 2013; Liu et al., 2013). This likely involves an ER docking site for OSBP1, VAP, which is targeted by interferon-inducible transmembrane protein 3 (IFITM3), leading to endosomal cholesterol accumulation and inhibition of enveloped virus entry (Amini-Bavil-Olyaee et al., 2013). We observed inhibition of HRV-A16 but not -A1A entry with 25-HC (Figure S5E), albeit at higher doses than blocking replication. Collectively, we conclude that rhinoviruses build up PI4P-rich Golgi membranes through PI4K3b to trigger lipid flux. We expect that other viruses than enteroviruses replicating on cytoplasmic membranes upregulate lipid signaling branches to generate membrane asymmetry that is critical for driving lipid counter-flux on replication membranes and thereby enhance viral replication.

EXPERIMENTAL PROCEDURES

Chemicals, plasmids and antibodies, cell lines, western blotting, reverse transcription PCR, image acquisitions, and analyses are described in Supplemental Information. Infections were at MOI 20, unless indicated otherwise. Figures were assembled using Adobe Photoshop and Illustrator. Graphs represent mean values of analyzed samples (n) including the SD and p values from t tests.

Primary Cells and Viruses
Human airway epithelial cells from nasal biopsies (hAECN) were cultured as recommended by the supplier (Epithelix, Geneva). HRV-A1A, -A2, -B14, -A16, -B37, and CVB3 were used as described (Jurgeit et al., 2010).

Lipid Extraction and Analyses
Phosphoinositides from HeLa cells were analyzed by ion chromatography with suppressed conductivity detection. Lipids were extracted into chloroform, dried, and fractionated by anion-exchange high-performance liquid chromatography (HPLC), and PI4P lipids were expressed as normalized to mitochondrial CL. For cholesterol and cholesteryl-ester analyses, HeLa-O cells were treated with inhibitors and infected with purified HRVs (MOI 50) in Dulbecco's modified Eagle's medium supplemented with 2% fetal bovine serum and 1% NEA at 37°C. Lipids were extracted into chloroform:methanol and analyzed in an Agilent HPLC 1100 system (Agilent) coupled with an Applied AB Sciex 3200 QTrap mass spectrometer (AB Sciex, Foster City). Cholesterol and cholesteryl-esters were separated by an Agilent Zorbax Eclipse XDB-C18 column, and their respective levels normalized to phospholipid levels.

Interference and High-Throughput Infection
siRNAs (20 nM) were reverse transfected to HeLa-O cells in 96-well plates using serum-free Opti-MEM (Invitrogen) and Lipofectamine RNAiMAX (Invitrogen) according to the manufacturer's protocol for 72 hr and infected with HRVs or CV at MOI 20 for 8 hr. Alternatively, cells were treated with chemical compounds, infected with HRV or CV, and scored for infection by immunostaining with mabJ2 or anti-VP2 antibodies. Images were acquired with an ImageXpress Micro microscope (Molecular Devices) in automated mode, using a CoolSNAP HQ 12bit gray scale camera (Roper Scientific) and 10×/NA 0.5 objective (Nikon), and analyzed with a custom-written script in Matlab (MathWorks, Inc., Natick). Infection indexes (fraction of infected cells per total cell number) were plotted with GraphPad Prism software (GraphPad) as relative units. Typically, infections under normal conditions yielded 30%–40% infected cells.

Immunofluorescence and Confocal Microscopy
HeLa-O cells on coverslips were treated 1 hr prior to infection with compounds or transfected with plasmid DNA using Lipofectamine 200 (Invitrogen) 24 hr prior to infection. Plasma membrane and cytoplasmic PI4P pools or other antigens were detected in cells fixed with 4% PFA and permeabilized with 0.2% Triton X-100, blocked for 1 hr in PBS supplemented with 1% bovine serum albumin (BSA), followed by primary IgM antibodies in blocking buffer overnight

at 4°C followed by Alexa Fluor-488 or -594 secondary antibodies for 1 hr. Cholesterol was stained with filipin in PBS for 30 min in cells fixed with 4% PFA. Coverslips were mounted in mounting medium (Dako) and analyzed with an inverted Leica TCS SP5 scanning laser confocal microscope with an HCX PL APO 63×/1.4 oil immersion objective. Images were acquired using LAS AF software (Leica) and processed with ImageJ (National Institutes of Health).

EM
Transmission EM of HeLa cells infected with HRV-A16 (MOI 1) for 15 hr at 33°C was carried out as described earlier (Strunze et al., 2011).

SUPPLEMENTAL INFORMATION

Supplemental Information includes five figures and Supplemental Experimental Procedures and can be found with this article online at http://dx.doi.org/10.1016/j.chom.2014.10.003.

REFERENCES

Amako, Y., Sarkeshik, A., Hotta, H., Yates, J., 3rd, and Siddiqui, A. (2009). Role of oxysterol binding protein in hepatitis C virus infection. J. Virol. *83*, 9237–9246.

Amini-Bavil-Olyaee, S., Choi, Y.J., Lee, J.H., Shi, M., Huang, I.C., Farzan, M., and Jung, J.U. (2013). The antiviral effector IFITM3 disrupts intracellular cholesterol homeostasis to block viral entry. Cell Host Microbe *13*, 452–464.

Arita, M., Kojima, H., Nagano, T., Okabe, T., Wakita, T., and Shimizu, H. (2013). Oxysterol-binding protein family I is the target of minor enviroxime-like compounds. J. Virol. *87*, 4252–4260.

Balla, T. (2013). Phosphoinositides: tiny lipids with giant impact on cell regulation. Physiol. Rev. *93*, 1019–1137.

Belov, G.A., and van Kuppeveld, F.J. (2012). (+)RNA viruses rewire cellular pathways to build replication organelles. Curr. Opin. Virol. *2*, 740–747.

Bianco, A., Reghellin, V., Donnici, L., Fenu, S., Alvarez, R., Baruffa, C., Peri, F., Pagani, M., Abrignani, S., Neddermann, P., and De Francesco, R. (2012). Metabolism of phosphatidylinositol 4-kinase IIIα-dependent PI4P Is subverted by HCV and is targeted by a 4-anilino quinazoline with antiviral activity. PLoS Pathog. *8*, e1002576.

Blanc, M., Hsieh, W.Y., Robertson, K.A., Kropp, K.A., Forster, T., Shui, G., Lacaze, P., Watterson, S., Griffiths, S.J., Spann, N.J., et al. (2013). The transcription factor STAT-1 couples macrophage synthesis of 25-hydroxycholesterol to the interferon antiviral response. Immunity 38, 106–118.

Bruckner, R.J., Mansy, S.S., Ricardo, A., Mahadevan, L., and Szostak, J.W. (2009). Flip-flop-induced relaxation of bending energy: implications for membrane remodeling. Biophys. J. 97, 3113–3122.

Burgett, A.W., Poulsen, T.B., Wangkanont, K., Anderson, D.R., Kikuchi, C., Shimada, K., Okubo, S., Fortner, K.C., Mimaki, Y., Kuroda, M., et al. (2011). Natural products reveal cancer cell dependence on oxysterol-binding proteins. Nat. Chem. Biol. 7, 639–647.

Carvou, N., Holic, R., Li, M., Futter, C., Skippen, A., and Cockcroft, S. (2010). Phosphatidylinositol- and phosphatidylcholine-transfer activity of PITPbeta is essential for COPI-mediated retrograde transport from the Golgi to the endoplasmic reticulum. J. Cell Sci. 123, 1262–1273.

de Saint-Jean, M., Delfosse, V., Douguet, D., Chicanne, G., Payrastre, B., Bourguet, W., Antonny, B., and Drin, G. (2011). Osh4p exchanges sterols for phosphatidylinositol 4-phosphate between lipid bilayers. J. Cell Biol. 195, 965–978.

Du, X., Kumar, J., Ferguson, C., Schulz, T.A., Ong, Y.S., Hong, W., Prinz, W.A., Parton, R.G., Brown, A.J., and Yang, H. (2011). A role for oxysterol-binding protein-related protein 5 in endosomal cholesterol trafficking. J. Cell Biol. 192, 121–135.

Farhan, H., Weiss, M., Tani, K., Kaufman, R.J., and Hauri, H.P. (2008). Adaptation of endoplasmic reticulum exit sites to acute and chronic increases in cargo load. EMBO J. 27, 2043–2054.

Gern, J.E. (2010). The ABCs of rhinoviruses, wheezing, and asthma. J. Virol. 84, 7418–7426.

Godi, A., Pertile, P., Meyers, R., Marra, P., Di Tullio, G., Iurisci, C., Luini, A., Corda, D., and De Matteis, M.A. (1999). ARF mediates recruitment of PtdIns-4-OH kinase-beta and stimulates synthesis of PtdIns(4,5)P2 on the Golgi complex. Nat. Cell Biol. 1, 280–287.

Goto, A., Liu, X., Robinson, C.A., and Ridgway, N.D. (2012). Multisite phosphorylation of oxysterol-binding protein regulates sterol binding and activation of sphingomyelin synthesis. Mol. Biol. Cell 23, 3624–3635.

Hashimoto, T., Segawa, H., Okuno, M., Kano, H., Hamaguchi, H.O., Haraguchi, T., Hiraoka, Y., Hasui, S., Yamaguchi, T., Hirose, F., and Osumi, T. (2012). Active involvement of micro-lipid droplets and lipid-droplet-associated proteins in hormone-stimulated lipolysis in adipocytes. J. Cell Sci. 125, 6127–6136.

Heaton, N.S., and Randall, G. (2011). Multifaceted roles for lipids in viral infection. Trends Microbiol. 19, 368–375.

Hsu, N.Y., Ilnytska, O., Belov, G., Santiana, M., Chen, Y.H., Takvorian, P.M., Pau, C., van der Schaar, H., Kaushik-Basu, N., Balla, T., et al. (2010). Viral reorganization of the secretory pathway generates distinct organelles for RNA replication. Cell 141, 799–811.

Hynynen, R., Suchanek, M., Spandl, J., Bäck, N., Thiele, C., and Olkkonen, V.M. (2009). OSBP-related protein 2 is a sterol receptor on lipid droplets that regulates the metabolism of neutral lipids. J. Lipid Res. 50, 1305–1315.

Ikonen, E. (2008). Cellular cholesterol trafficking and compartmentalization. Nat. Rev. Mol. Cell Biol. 9, 125–138.

Ilnytska, O., Santiana, M., Hsu, N.Y., Du, W.L., Chen, Y.H., Viktorova, E.G., Belov, G., Brinker, A., Storch, J., Moore, C., et al. (2013). Enteroviruses harness the cellular endocytic machinery to remodel the host cell cholesterol landscape for effective viral replication. Cell Host Microbe 14, 281–293.

Jacobs, S.E., Lamson, D.M., St George, K., and Walsh, T.J. (2013). Human rhinoviruses. Clin. Microbiol. Rev. 26, 135–162.

Jurgeit, A., Moese, S., Roulin, P., Dorsch, A., Lötzerich, M., Lee, W.-M., and Greber, U.F. (2010). An RNA replication-center assay for high content image-based quantifications of human rhinovirus and coxsackievirus infections. Virol. J. 7, 264.

Jurgeit, A., McDowell, R., Moese, S., Meldrum, E., Schwendener, R., and Greber, U.F. (2012). Niclosamide is a proton carrier and targets acidic endosomes with broad antiviral effects. PLoS Pathog. 8. Published online October 25, 2014. http://dx.doi.org/10.1371/journal.ppat.1002976.

Kandutsch, A.A., and Chen, H.W. (1974). Inhibition of sterol synthesis in cultured mouse cells by cholesterol derivatives oxygenated in the side chain. J. Biol. Chem. 249, 6057–6061.

Knight, Z.A., Gonzalez, B., Feldman, M.E., Zunder, E.R., Goldenberg, D.D., Williams, O., Loewith, R., Stokoe, D., Balla, A., Toth, B., et al. (2006). A pharmacological map of the PI3-K family defines a role for p110alpha in insulin signaling. Cell 125, 733–747.

Liu, S.Y., Aliyari, R., Chikere, K., Li, G., Marsden, M.D., Smith, J.K., Pernet, O., Guo, H., Nusbaum, R., Zack, J.A., et al. (2013). Interferon-inducible cholesterol-25-hydroxylase broadly inhibits viral entry by production of 25-hydroxycholesterol. Immunity 38, 92–105.

Manna, P.R., Cohen-Tannoudji, J., Counis, R., Garner, C.W., Huhtaniemi, I., Kraemer, F.B., and Stocco, D.M. (2013). Mechanisms of action of hormone-sensitive lipase in mouse Leydig cells: its role in the regulation of the steroidogenic acute regulatory protein. J. Biol. Chem. 288, 8505–8518.

Mello, C., Aguayo, E., Rodriguez, M., Lee, G., Jordan, R., Cihlar, T., and Birkus, G. (2014). Multiple classes of antiviral agents exhibit in vitro activity against human rhinovirus type C. Antimicrob. Agents Chemother. 58, 1546–1555.

Mesmin, B., Bigay, J., Moser von Filseck, J., Lacas-Gervais, S., Drin, G., and Antonny, B. (2013). A four-step cycle driven by PI(4)P hydrolysis directs sterol/PI(4)P exchange by the ER-Golgi tether OSBP. Cell 155, 830–843.

Olkkonen, V.M., and Li, S. (2013). Oxysterol-binding proteins: sterol and phosphoinositide sensors coordinating transport, signaling and metabolism. Prog. Lipid Res. 52, 529–538.

Raychaudhuri, S., and Prinz, W.A. (2010). The diverse functions of oxysterol-binding proteins. Annu. Rev. Cell Dev. Biol. 26, 157–177.

Reiss, S., Rebhan, I., Backes, P., Romero-Brey, I., Erfle, H., Matula, P., Kaderali, L., Poenisch, M., Blankenburg, H., Hiet, M.S., et al. (2011). Recruitment and activation of a lipid kinase by hepatitis C virus NS5A is essential for integrity of the membranous replication compartment. Cell Host Microbe 9, 32–45.

Rocha, N., Kuijl, C., van der Kant, R., Janssen, L., Houben, D., Janssen, H., Zwart, W., and Neefjes, J. (2009). Cholesterol sensor ORP1L contacts the ER protein VAP to control Rab7-RILP-p150 Glued and late endosome positioning. J. Cell Biol. 185, 1209–1225.

Romeo, G.R., and Kazlauskas, A. (2008). Oxysterol and diabetes activate STAT3 and control endothelial expression of profilin-1 via OSBP1. J. Biol. Chem. 283, 9595–9605.

Sharp, T.M., and Estes, M.K. (2010). An inside job: subversion of the host secretory pathway by intestinal pathogens. Curr. Opin. Infect. Dis. 23, 464–469.

Spickler, C., Lippens, J., Laberge, M.K., Desmeules, S., Bellavance, E., Garneau, M., Guo, T., Hucke, O., Leyssen, P., Neyts, J., et al. (2013). Phosphatidylinositol 4-kinase III beta is essential for replication of human rhinovirus and its inhibition causes a lethal phenotype in vivo. Antimicrob. Agents Chemother. 57, 3358–3368.

Spooner, R.A., Watson, P., Smith, D.C., Boal, F., Amessou, M., Johannes, L., Clarkson, G.J., Lord, J.M., Stephens, D.J., and Roberts, L.M. (2008). The secretion inhibitor Exo2 perturbs trafficking of Shiga toxin between endosomes and the trans-Golgi network. Biochem. J. 414, 471–484.

Strunze, S., Engelke, M.F., Wang, I.-H., Puntener, D., Boucke, K., Schleich, S., Way, M., Schoenenberger, P., Burckhardt, C.J., and Greber, U.F. (2011). Kinesin-1-mediated capsid disassembly and disruption of the nuclear pore complex promote virus infection. Cell Host Microbe 10, 210–223.

Suomalainen, M., and Greber, U.F. (2013). Uncoating of non-enveloped viruses. Curr. Opin. Virol. 3, 27–33.

Suomalainen, M., Nakano, M.Y., Boucke, K., Keller, S., and Greber, U.F. (2001). Adenovirus-activated PKA and p38/MAPK pathways boost microtubule-mediated nuclear targeting of virus. EMBO J. 20, 1310–1319.

van der Schaar, H.M., Leyssen, P., Thibaut, H.J., de Palma, A., van der Linden, L., Lanke, K.H., Lacroix, C., Verbeken, E., Conrath, K., Macleod, A.M., et al. (2013). A novel, broad-spectrum inhibitor of enterovirus replication that targets host cell factor phosphatidylinositol 4-kinase IIIβ. Antimicrob. Agents Chemother. *57*, 4971–4981.

Walther, T.C., and Farese, R.V., Jr. (2012). Lipid droplets and cellular lipid metabolism. Annu. Rev. Biochem. *81*, 687–714.

Wang, Y.J., Wang, J., Sun, H.Q., Martinez, M., Sun, Y.X., Macia, E., Kirchhausen, T., Albanesi, J.P., Roth, M.G., and Yin, H.L. (2003). Phosphatidylinositol 4 phosphate regulates targeting of clathrin adaptor AP-1 complexes to the Golgi. Cell *114*, 299–310.

Wang, P.Y., Weng, J., Lee, S., and Anderson, R.G. (2008). The N terminus controls sterol binding while the C terminus regulates the scaffolding function of OSBP. J. Biol. Chem. *283*, 8034–8045.